

PHONON AND POLARON STATES OF ZnO/GaN AND GaN/AlN CYLINDRICAL WIRES

V.I. BOICHUK, L.YA. VORONYAK, YA.M. VORONYAK

PACS 71.55.-i, 73.21.La,
79.60.Jv
©2011

Ivan Franko Drohobych State Pedagogical University
(3, Stryiska Str., Drohobych 82100, Ukraine; e-mail: voronyak.lyubov@gmail.com)

The energy of polarization phonons as a function of the wave vector as well as the polaron energy and effective mass as functions of the quantum wire radius R are determined for cylindrical quantum wires (QWs) of ZnO and GaN hexagonal crystals. It is shown that the dominant contribution to the polaron energy and the effective mass is made by quasi-longitudinal and interface phonon modes. It is established that the contribution of quasi-longitudinal phonons is determinative in the region $R > 15$ nm. The energies of QW polarons for cubic and hexagonal crystals are compared.

DCM to theoretically analyze the properties of optical phonons and their interaction with a conduction electron in various heterostructures of wurtzite-like crystals with plane boundaries [18, 22, 23]. Much less studied (both experimentally and theoretically) are the phonon and polaron states in quantum wires and quantum dots of anisotropic crystals [19–21, 24].

The proposed work is devoted to the theoretical research of the phonon and polaron states in quantum wires of anisotropic ZnO and GaN crystals in ZnO/GaN and GaN/AlN heterostructures.

1. Introduction

The general development of semiconductor nanotechnologies observed during two recent decades allows one to make a conclusion about the importance of the electron – optical phonon interaction in low-dimensional systems. In such systems, electron-phonon interaction can significantly influence the physical properties of electrons, in particular, their scattering, energy losses of hot electrons, polaron effects, *etc.* [1–10]. This so-called Fröhlich interaction is mainly studied in the framework of the dielectric continuum model (DCM). Its use allows one to obtain expressions for the investigated parameters in relatively simple analytical forms. In addition, the results obtained in the framework of this model are in good agreement with experimental data [1, 8, 11–14].

First, electron – optical phonon interaction was thoroughly studied in quasi-two-dimensional heterosystems, quantum wires, and quantum dots produced using optically isotropic materials [14–17]. However, during the recent years, such anisotropic materials as ZnO, GaN, AlN, and InN have started to attract attention of investigators due to perspectives of their use in electronics [18–24]. In particular, a number of studies have used the

2. Statement of the Problem and Its Solution

We consider a nanoheterostructure consisting of a cylindrical quantum wire of radius R in the semiconductor matrix of wurtzite-like crystals. The axis OZ is directed along the wire axis that coincides with the optical axis of the crystals \mathbf{c} (Fig. 1).

In the effective mass and dielectric continuum approximations, the electron-phonon system is described by the Hamiltonian

$$\hat{H} = \hat{H}_e + \hat{H}_{ph} + \hat{H}_{e-ph}. \tag{1}$$

The Hamiltonian of the electron subsystem \hat{H}_e can be put down in the coordinate representation using the cylindrical system of coordinates

$$\hat{H}_e = -\frac{\hbar^2}{2} \left(\frac{1}{\rho} \frac{\partial}{\partial \rho} \left(\frac{\rho}{m_t(\rho)} \frac{\partial}{\partial \rho} \right) + \frac{1}{\rho^2} \frac{\partial^2}{\partial \varphi^2} + \frac{1}{m_z(\rho)} \frac{\partial^2}{\partial z^2} \right) + V(\rho), \tag{2}$$

where

$$m_{z(t)}(\rho) = \begin{cases} m_{1,z(t)}, & 0 \leq \rho < R, \\ m_{2,z(t)}, & R \leq \rho < \infty \end{cases} \quad (3)$$

are the axial ($m_{i,z}$) and radial ($m_{i,t}$) effective electron masses and

$$V(\rho) = \begin{cases} -V, & 0 \leq \rho < R, \\ 0, & R \leq \rho < \infty, \end{cases} \quad V = U_1 - U_2 \quad (4)$$

is the potential of the cylindrical quantum well. Here, U_i is the electron potential energy in the bulky medium with respect to vacuum. Indices 1 and 2 correspond to the internal and external media of the heterosystem, respectively. The eigenfunctions and eigenvalues of the electron Hamiltonian have the following form:

$$\Psi_{N,M,k}(\rho, \varphi, z) = \frac{A_{N,M}}{\sqrt{2\pi L}} \phi_{N,M}(\rho) e^{ikz + iM\varphi}, \quad (5)$$

$$\phi_{N,M}(\rho) = \begin{cases} J_{|M|}(\kappa_{1,N,M}\rho), & 0 \leq \rho < R, \\ \frac{J_{|M|}(\kappa_{1,N,M}R)}{K_{|M|}(\kappa_{2,N,M}R)} K_{|M|}(\kappa_{2,N,M}\rho), & R \leq \rho < \infty, \end{cases} \quad (6)$$

$$\kappa_{2,N,M} = \sqrt{\frac{2m_{2,t}V}{\hbar^2} - \frac{m_{2,t}\kappa_{1,N,M}^2}{m_{1,t}}} \quad (7)$$

$$|A_{N,M}|^2 = -2 / \left(R^2 \left(J_{|M|-1}(\kappa_{1,N,M}R) J_{|M|+1}(\kappa_{1,N,M}R) - \frac{J_{|M|}(\kappa_{1,N,M}R)^2 K_{|M|-1}(\kappa_{2,N,M}R) K_{|M|+1}(\kappa_{2,N,M}R)}{K_{|M|}(\kappa_{2,N,M}R)^2} \right) \right), \quad (8)$$

$$E_{N,M}(k) = -V + \frac{\hbar^2 \kappa_{1,N,M}^2}{2m_{1,t}} + \frac{\hbar^2 k^2}{2m_{1,z}}, \quad (9)$$

where k is the axial component of the electron wave vector, $\kappa_{1,N,M}$ are the roots of the dispersion equation

$$\begin{aligned} & \frac{\kappa_1 (J_{|M|-1}(\kappa_1 R) - J_{|M|+1}(\kappa_1 R))}{m_{1,t} J_{|M|}(\kappa_1 R)} = \\ & = \frac{\kappa_2 (-K_{|M|-1}(\kappa_2 R) - K_{|M|+1}(\kappa_2 R))}{m_{2,t} K_{|M|}(\kappa_2 R)}. \end{aligned} \quad (10)$$

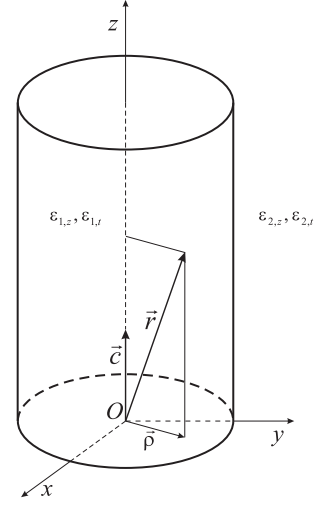


Fig. 1. Diagram of a cylindrical quantum wire in the semiconductor matrix

$N = 1, 2, \dots, N_{\max}(R)$ and $M = 0, \pm 1, \pm 2, \dots, \pm M_{\max}(R)$ stand for the radial and magnetic quantum numbers, respectively, $J_M(x)$ are the cylindrical Bessel functions, and $K_M(x)$ are the modified Bessel functions. The Hamiltonian of the phonon subsystem \hat{H}_{ph} can be written down in the representation of occupation numbers with respect to the phonon variables

$$\begin{aligned} \hat{H}_{\text{ph}} &= \sum_s \hat{H}_s = \\ &= \sum_s \sum_{m_s, n_s, q} \hbar \omega_{s, m_s, n_s}(q) \left(b_{s, m_s, n_s, q}^+ b_{s, m_s, n_s, q} + \frac{1}{2} \right), \end{aligned} \quad (11)$$

where $b_{s, m_s, n_s, q}^+$ ($b_{s, m_s, n_s, q}$) is the operator of creation (annihilation) of a polarization phonon of the (s, m_s, n_s, q) branch. The index s corresponds to the type of polarization phonons, $n_s = 1, 2, \dots$ and $m_s = 0, \pm 1, \pm 2, \dots$ are the radial and magnetic quantum numbers, respectively, whereas q is the axial component of the wave vector. The spectrum of polarization phonons $\hbar \omega_{s, m_s, n_s}(q)$ is determined from the dispersion equation

$$\left(\frac{\gamma_1 \varepsilon_{1,t}}{\gamma_2 \varepsilon_{2,t}} - \frac{Z_{1,s,|m|}(\gamma_1 q R) Z'_{2,s,|m|}(\gamma_2 q R)}{Z_{2,s,|m|}(\gamma_2 q R) Z'_{1,s,|m|}(\gamma_1 q R)} \right) = 0, \quad (12)$$

where

$$Z'_{i,s,|m|}(x) = \frac{d}{dx} Z_{i,s,|m|}(x), \quad \gamma_i = \sqrt{\left| \frac{\varepsilon_{i,z}(\omega)}{\varepsilon_{i,t}(\omega)} \right|},$$

$$\varepsilon_{i,z}(\omega) = \varepsilon_{i,z,\infty} \frac{(\omega_{\text{LOz},i}^2 - \omega^2)}{\omega_{\text{TOz},i}^2 - \omega^2},$$

$$\varepsilon_{i,t}(\omega) = \varepsilon_{i,t,\infty} \frac{(\omega_{\text{LOt},i}^2 - \omega^2)}{\omega_{\text{TOt},i}^2 - \omega^2} \quad (13)$$

stand for the axial and radial components of the permittivity tensor of the internal (quantum wire, $i = 1$) and external (matrix, $i = 2$) media, respectively.

The functions $Z_{i,s,|m|}$ are expressed in terms of the Bessel $J_M(x)$, Neumann $Y_M(x)$, and modified Bessel functions of the first, $I_M(x)$, and second, $K_M(x)$, kinds as

$$Z_{1,\text{IO},|m|}(x) = I_{|m|}(x), \quad Z_{2,\text{IO},|m|}(x) = K_{|m|}(x),$$

$$Z_{1,\text{QC},|m|}(x) = J_{|m|}(x), \quad Z_{2,\text{QC},|m|}(x) = K_{|m|}(x),$$

$$Z_{1,\text{EC},|m|}(x) = J_{|m|}(x), \quad Z_{2,\text{EC},|m|}(x) = 0,$$

$$Z_{1,\text{HSL},|m|}(x) = I_{|m|}(x),$$

$$Z_{2,\text{HSL},|m|}(x) = J_{|m|}(x) - \frac{J_{|m|}(qzR_\infty\gamma_1)}{Y_{|m|}(qzR_\infty\gamma_2)} Y_{|m|}(x) \quad (14)$$

for interface (interface optical, IO), confined (QC), exactly confined (EC), and half-space-like (HSL) phonons, respectively. $R_\infty \gg R$ is the radius of the dielectric matrix.

The investigated nanoheterostructures of wurtzite semiconductors have two branches of IO-, QC-, and HSL-phonons, whose frequencies lie in the following intervals:

IO-phonons:

$$\varepsilon_{1,z}(\omega)\varepsilon_{1,t}(\omega) > 0, \quad \varepsilon_{2,z}(\omega)\varepsilon_{2,t}(\omega) > 0, \quad \varepsilon_{1,t}(\omega) > 0,$$

$$\varepsilon_{2,t}(\omega) < 0, \quad \omega_{\text{TOt},1} < \omega < \omega_{\text{TOz},2}$$

– quasi-transverse phonons (IOT),

$$\varepsilon_{1,z}(\omega)\varepsilon_{1,t}(\omega) > 0, \quad \varepsilon_{2,z}(\omega)\varepsilon_{2,t}(\omega) > 0, \quad \varepsilon_{1,t}(\omega) < 0,$$

$$\varepsilon_{2,t}(\omega) > 0, \quad \omega_{\text{LOt},1} < \omega < \omega_{\text{LOz},2}$$

– quasi-longitudinal phonons (IOL). The spectrum of IO phonons does not depend on the radial quantum number. Therefore, we consider in what follows that $n_{\text{IO}} = 1$.

QC-phonons:

$$\varepsilon_{1,z}(\omega)\varepsilon_{1,t}(\omega) < 0, \quad \varepsilon_{2,z}(\omega)\varepsilon_{2,t}(\omega) > 0, \quad \varepsilon_{1,t}(\omega) > 0,$$

$$\omega_{\text{TOz},1} < \omega < \omega_{\text{TOt},1}$$

– quasi-transverse phonons (QCT),

$$\varepsilon_{1,z}(\omega)\varepsilon_{1,t}(\omega) < 0, \quad \varepsilon_{2,z}(\omega)\varepsilon_{2,t}(\omega) > 0, \quad \varepsilon_{1,z}(\omega) > 0,$$

$$\omega_{\text{LOz},1} < \omega < \omega_{\text{LOt},1}$$

– quasi-longitudinal phonons (QCL).

HSL-phonons:

$$\varepsilon_{1,z}(\omega)\varepsilon_{1,t}(\omega) > 0, \quad \varepsilon_{2,z}(\omega)\varepsilon_{2,t}(\omega) < 0, \quad \varepsilon_{2,t}(\omega) > 0,$$

$$\omega_{\text{TOz},2} < \omega < \omega_{\text{TOt},2}$$

– quasi-transverse phonons (HSLT),

$$\varepsilon_{1,z}(\omega)\varepsilon_{1,t}(\omega) > 0, \quad \varepsilon_{2,z}(\omega)\varepsilon_{2,t}(\omega) < 0, \quad \varepsilon_{2,z}(\omega) > 0,$$

$$\omega_{\text{LOz},2} < \omega < \omega_{\text{LOt},2}$$

– quasi-longitudinal phonons (HSLL).

The frequency of EC phonons is determined from the condition

$$\varepsilon_{1,t}(\omega) = 0, \quad \omega = \omega_{\text{LOt},1}.$$

The interaction of an electron with polarization phonons is described by the Hamiltonian of the form

$$\hat{H}_{e\text{-ph}} = - \sum_s \sum_{m_s, n_s, q} \Gamma_{s, m_s, n_s}(q) \times$$

$$\times \left(\frac{1}{\sqrt{2\pi L}} Z_{s, m_s}(\rho) e^{iqz} e^{im_s\varphi} b_{s, m_s, n_s, q} + \text{h.c.} \right), \quad (15)$$

where

$$\Gamma_{s, m_s, n_s}(q) = \frac{1}{\sqrt{2\pi L}} \sqrt{\frac{\hbar e^2}{2\varepsilon_0\omega}}$$

$$\times \left(\int_0^R F_{1, s, m_s}(\rho) \rho d\rho + B_{s, m_s}^2 \int_R^\infty F_{2, s, m_s}(\rho) \rho d\rho \right)^{-2}, \quad (16)$$

$$Z_{s,m_s}(\rho) = \begin{cases} Z_{1,s,m_s}(\gamma_1 q \rho), & 0 \leq \rho < R, \\ B_{s,m_s} Z_{2,s,m_s}(\gamma_2 q \rho), & R \leq \rho < \infty, \end{cases} \quad (17)$$

$$B_{s,m_s} = \frac{Z_{1,s,m_s}(\gamma_1 q R)}{Z_{2,s,m_s}(\gamma_2 q R)}, \quad (18)$$

$$F_{i,s,m_s}(\rho) = \left(\left(\frac{m_s^2}{g_{i,t}^2 \rho^2} + \frac{q^2}{g_{i,z}^2} \right) Z_{i,s,m_s}^2(\gamma_i q \rho) + \frac{\gamma_i^2 q^2 (Z'_{i,s,m_s}(\gamma_i q \rho))^2}{g_{i,t}^2} \right), \quad (19)$$

$$g_{i,t} = \sqrt{\frac{(\omega^2 - \omega_{\text{TO}t,i}^2)^2}{\varepsilon_{i,t,\infty}(\omega_{\text{LO}t,i}^2 - \omega_{\text{TO}t,i}^2)}},$$

$$g_{i,z} = \sqrt{\frac{(\omega^2 - \omega_{\text{TO}z,i}^2)^2}{\varepsilon_{i,z,\infty}(\omega_{\text{LO}z,i}^2 - \omega_{\text{TO}z,i}^2)}}, \quad (20)$$

ε_0 stands for the dielectric constant, while $\varepsilon_{i,z,\infty}$ and $\varepsilon_{i,t,\infty}$ are the high-frequency axial and radial components of the permittivity tensor of bulky crystals.

Let us investigate the renormalization of the electron ground-state energy due to the interaction of a charge with polarization oscillations. In the

case of weak coupling, the latter is specified by the second correction of the perturbation theory:

$$E_{\text{pol}}(k) = E_{1,0}(k) + \sum_{N,M,s,n_s,q} \frac{|\langle 1_{ph,s,n_s,M,q} | \langle \Psi_{N,-M,k-q} | H_{e-ph} | \Psi_{1,0,k} \rangle | 0_{\text{ph}} \rangle|^2}{E_{1,0}(k) - E_{N,-M}(k) - \hbar \omega_{M,n_s}(q)}, \quad (21)$$

where $|\Psi_{1,0,k}\rangle | 0_{\text{ph}}\rangle$ is the wave function of the ground (vacuum) state of the system and $|\Psi_{N,-M,k-q}\rangle | 1_{ph,s,n_s,M,q}\rangle$ are the wave functions of its intermediate (excited) states.

For extreme values of the vector \mathbf{k} , the energy $E_{\text{pol}}(\mathbf{k})$ can be expanded into a series introducing the effective polaron mass:

$$E_{\text{pol}}(k) = E_{\text{pol}}(0) + \frac{\hbar^2 k^2}{2m_{\text{pol}}}, \quad (22)$$

$$\frac{1}{m_{\text{pol}}} = \frac{1}{\hbar^2} \left(\frac{\partial^2}{\partial k^2} E_{\text{pol}}(k) \right)_{k=0}, \quad (23)$$

$$E_{\text{pol}}(0) = E_{1,0}(0) + \Delta E_{\text{pol}}(0) = \frac{\hbar^2 \kappa_{1,1,0}^2}{2m_{1,t}} + \sum_s \Delta E_s, \quad (24)$$

$$\Delta E_s = \sum_{N,M,n_s,q} \left(-\frac{1}{2\pi L} \frac{|G_{s,N,M,n_s}(q)|^2}{\hbar \omega_{s,M,n_s}(q) + \frac{\hbar^2 q^2}{2m_{1,z}} + \frac{\hbar^2 \kappa_{1,N,M}^2}{2m_{1,t}} - \frac{\hbar^2 \kappa_{1,1,0}^2}{2m_{1,t}}} \right), \quad (25)$$

$$m_{\text{pol}} = \frac{m_{1,z}}{\left(1 - 4 \left(\frac{2m_{1,z}}{\hbar^2} \right)^2 \frac{1}{2\pi L} \sum_{s,N,M,n_s,q} \frac{q^2 |G_{s,N,M,n_s}(q)|^2}{\left(\left(q^2 + \frac{2m_{1,z}}{\hbar^2} \hbar \omega_{s,M,n_s}(q) \right) + \frac{m_{1,z}}{m_{1,t}} (\kappa_{1,N,M}^2 - \kappa_{1,1,0}^2) \right)^3} \right)}, \quad (26)$$

$$-\frac{G_{s,N,M,n_s}(q)}{\sqrt{2\pi L}} = \langle 1_{ph,s,M,n_s,q} | \langle \Psi_{N,-M,k-q} | H_{e-ph} | \Psi_{1,0,k} \rangle | 0_{\text{ph}} \rangle = \int_0^\infty \phi_{N,M}(\rho) \Gamma_{s,M,n_s}(q) Z_{s,M}(\rho) \phi_{1,0}(\rho) \rho d\rho. \quad (27)$$

	$\hbar\omega_{\text{TOz}}, \text{cm}^{-1}$	$\hbar\omega_{\text{TOt}}, \text{cm}^{-1}$	$\hbar\omega_{\text{LOz}}, \text{cm}^{-1}$	$\hbar\omega_{\text{LOt}}, \text{cm}^{-1}$	ε_z	ε_t	m_z/m_0	m_t/m_0	U_i, eV
ZnO	380	413	579	591	3.78	3.7	0.27	0.27	4.77
GaN	533	561	735	743	5.29	5.29	0.2	0.2	4.1
AlN	660	673	893	916	4.68	4.68	0.4	0.4	0.6

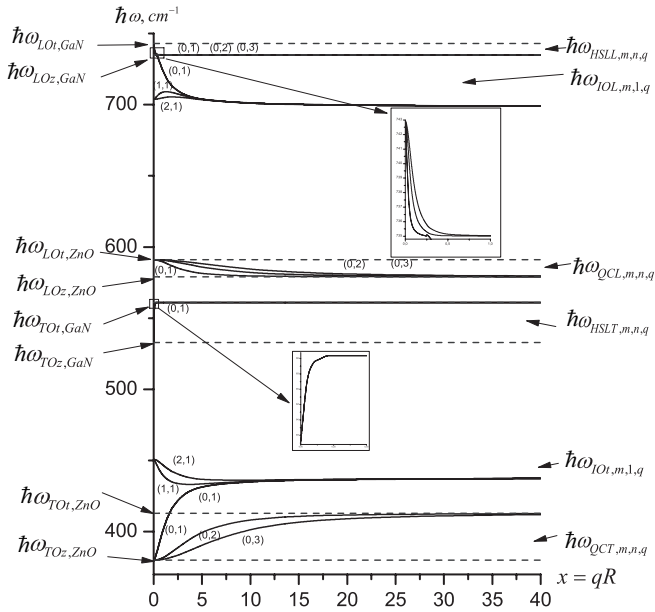


Fig. 2. Spectrum of polarization phonons for the ZnO/GaN structure

3. Analysis of the Obtained Results

The phonon energy, polaron energy $E_{\text{pol}}(0)$, and polaron effective mass were calculated for the ZnO/GaN and GaN/AlN heterostructures. The parameters of the corresponding crystals are listed in Table.

The energy spectra of polarization phonons of the ZnO/GaN and GaN/AlN cylindrical heterosystems are presented in Figs. 2 and 3. Due to the fact that these heterostructures are formed by hexagonal crystals, the states of HSL ($\hbar\omega_{\text{HSLT}}, \hbar\omega_{\text{HSL}}$) and QC ($\hbar\omega_{\text{QCL}}, \hbar\omega_{\text{QCT}}$) phonons in the region $q > 0$ are non-degenerate. It is worth noting that the analogous states of heterosystems based on cubic crystals are degenerate, and the energies of the indicated phonons coincide with those of the corresponding phonons of the crystals forming the matrix (for HSL phonons) or the wire (for QC ones) for any value of the wave vector [4, 6].

A thorough analysis of $\hbar\omega_{\text{HSL}}(q)$ and $\hbar\omega_{\text{HSLT}}(q)$ demonstrates that these functions assume various values at fixed q in a small range of variation of the wave vector: $0 < qR \leq \alpha$. As one can see from the figures, the

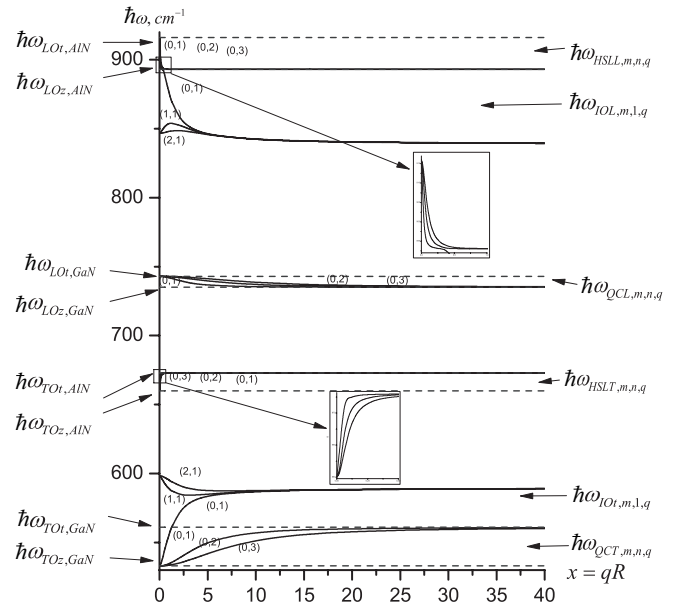


Fig. 3. Spectrum of polarization phonons for the GaN/AlN structure

width of this region (α) depends not only on the kind of the heterostructure but also on the type of phonons (HSL or HSLT). In the region $qR > \alpha$, the energy of quasi-longitudinal (HSL) phonons practically coincides with that of longitudinal optical phonons of the matrix $\hbar\omega_{\text{LOz}}$, and the energy of quasi-transverse (HSLT) phonons is almost the same as that of transverse phonons of the matrix $\hbar\omega_{\text{TOt}}$. Confined polarization phonons are characterized by a different dispersion dependence. The energies of both quasi-longitudinal (QCL) and quasi-transverse (QCT) phonons depend on m and n in the whole range of variation of qR .

Another peculiarity of the energy spectrum of polarization phonons in the considered heterostructures is that the (0,1) branch of HSL phonons continuously passes into the (0,1) branch of IOL ones. Similarly, the (0,1) branch of QCT phonons passes into the (0,1) branch of IOT phonons.

Interface phonons (both IOL and IOT ones) are characterized by different dispersion branches (m, n) that practically coincide in the region of large qR ($qR > 0$). The energy of these phonons is determined by the energy

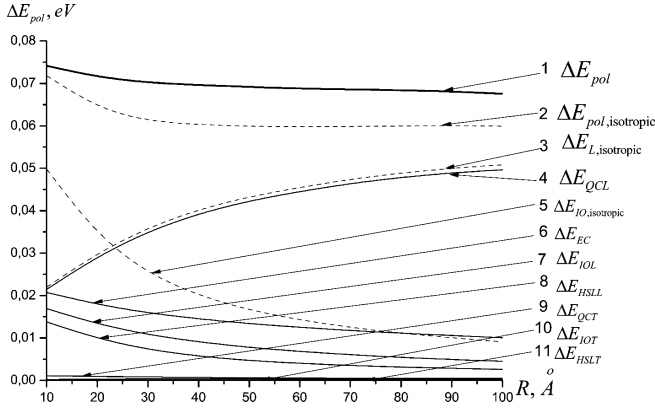


Fig. 4. Partial contributions to the polaron energy for the ZnO/GaN structure

of optical phonons of both the matrix and the quantum wire:

$$\hbar\omega_{\text{LO}z2} \leq \hbar\omega_{\text{IOL}} < \hbar\omega_{\text{LO}t1}, \quad \hbar\omega_{\text{TO}t1} \leq \hbar\omega_{\text{IOT}} < \hbar\omega_{\text{TO}z2}.$$

One more type of phonons existing in the “quantum wire – matrix” heterosystem of anisotropic crystals is exactly confined (EC) phonons, whose wave vector equals zero and $\hbar\omega_{\text{EC}} = \hbar\omega_{\text{LO}t1}$.

Figures 4 and 5 illustrate the dependence of the polaron coupling energy $\Delta E_{\text{pol}} = E_{10}(0) - E_{\text{pol}}(0)$ ($E_{\text{pol}}(0)$ denotes the polaron energy at $\mathbf{k} = \mathbf{0}$, while $E_{10}(0)$ is the electron ground-state energy) on the QW radius of the ZnO/GaN (Fig. 4) and GaN/AlN (Fig. 5) heterostructures. One can see that the partial contribution to the polaron energy depends on the type of polarization phonons. Particularly, the contribution of quasi-transverse phonons (QCT, IOT, and HSLT) is rather small (< 1 meV) for all the considered QW radii ($R \geq 10$ Å). The contribution of half-space-like, interface, and exactly confined phonons in the region $R \in [10 \text{ Å}, 100 \text{ Å}]$ varies from several to tens of millielectronvolts. Moreover, a decrease of R is accompanied by an increase of the contribution of these phonons into the polaron energy, which is explained by the intensification of the electron interaction with the corresponding phonon modes. The radial dependence of the partial contribution made to ΔE_{pol} by confined phonons behaves in a different way. One can see that, with decreasing R , this quantity (curve 4) monotonously reduces. The summation of all contributions to the polaron coupling energy yields a monotonous increase of ΔE_{pol} in the whole range of variation of R (curve 1).

Figures 4 and 5 also present the dependence of the polaron coupling energy in QW heterostructures of

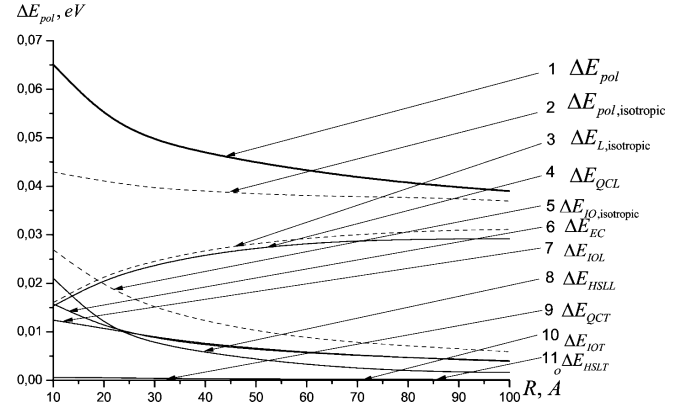


Fig. 5. Partial contributions to the polaron energy for the GaN/AlN structure

isotropic ZnO, GaN, and AlN crystals (curve 2). The parameters for these crystals were chosen as arithmetical means of the corresponding parameters of anisotropic crystals:

$$\omega_{\text{LO}} = \frac{1}{2}(\omega_{\text{LO}t} + \omega_{\text{LO}z});$$

$$\omega_{\text{TO}} = \frac{1}{2}(\omega_{\text{TO}t} + \omega_{\text{TO}z});$$

$$\varepsilon_{\infty} = \frac{1}{2}(\varepsilon_{t,\infty} + \varepsilon_{z,\infty}).$$

The partial contributions made to the energy ΔE_{pol} by interface (curve 5) and confined (curve 3) phonons are determinative. The contribution of HSL phonons is rather small and not shown in the figure. The behavior of the dependence $\Delta E_{\text{pol}} = \Delta E(R)$ for the indicated types of phonons is qualitatively the same for the both symmetry types of the crystals: the contribution of interface phonons increases with decrease in the QW radius, while that of confined ones – decreases. After the summation, the polaron coupling energy of cubic crystals monotonously increases, as R decreases. As one can see from Fig. 4, the difference between the energies ΔE_{pol} of ZnO/GaN heterostructures of anisotropic and isotropic crystals in the region of small R approximates ~ 2 meV at $R = 10$ Å. An increase of R results in the growth of this difference which almost does not depend on R in the region $R > 100$ Å. The obtained value coincides with the energy difference ΔE_{pol} for ZnO bulky crystals. In the case of GaN/AlN heterostructures (Fig. 5), a growth of R results in the monotonous approach of the difference between the polaron energies to the energy difference ΔE_{pol} for bulky isotropic and anisotropic GaN crystals.

As is noted above, a decrease of R induces the intensification of the electron-phonon interaction in QWs.

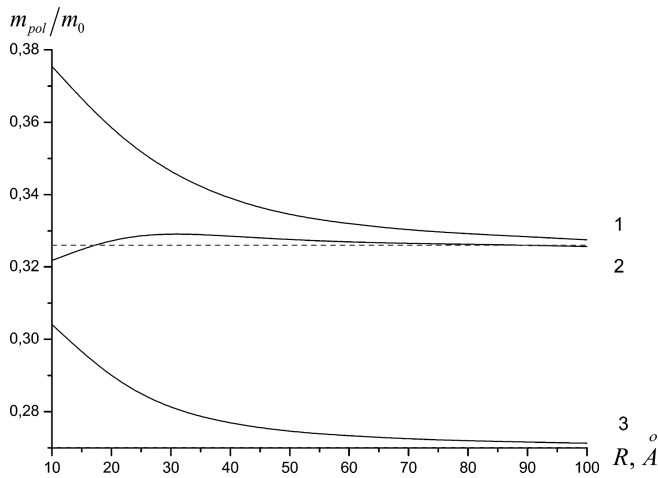


Fig. 6. Effective polaron mass as a function of the QW radius for the ZnO/GaN structure

This effect can be also observed considering the dependence of the polaron effective mass on the QW radius of the ZnO/GaN heterosystem (Fig. 6). Our calculations demonstrate that a decrease of R is accompanied by an increase of the polaron effective mass (curve 1) and $m_{\text{pol}} = 0.375m_0$ at $R = 10 \text{ \AA}$ is the free electron mass). At $R = 100 \text{ \AA}$, the polaron mass in the heterosystem almost coincides with that in the bulky ZnO crystal (dotted line) according to the formula

$$m_{\text{pol}} = \frac{m_0}{1 - \alpha_0/6}, \quad (28)$$

where α_0 is the Fröhlich constant.

It is also obtained that the dominant contribution to m_{pol} is made by confined and interface phonons. With regard for only confined and exactly confined phonons, the dependence $m_{\text{pol}} = m_{\text{pol}}(R)$ is specified by curve 2. It is seen that, at $R > 60 \text{ \AA}$, the effect of these phonons on the formation of m_{pol} is determinative. If only interface phonons are taken into account, the dependence of the polaron effective mass on R is described by curve 3. One can see that these phonons are significant at $R < 40 \text{ \AA}$.

Based on the performed calculations, a conclusion can be made that taking the anisotropy of GaN and AlN crystals into account makes corrections to the energy of polarization phonons, energy of polaron states, and polaron effective mass as compared to the cubic crystal model. The obtained energies of interface, confined, and half-space-like phonons can be used for the analysis of Raman spectra of GaN/AlN and ZnO/GaN heterosystems with quantum wires. Moreover, according to the

calculation results, the coupling energy of an electron polaron for the model of anisotropic semiconductors in the considered region of QW radii is 10% ÷ 15% larger than that in the isotropic model. An analogous result is obtained for a hole polaron. Thus, taking the anisotropy into account refines the energy of interband transitions, which must affect the energies of exciton absorption and luminescence [25, 26].

4. Conclusions

The work reports on the investigation of the ground state of an electron polaron in ZnO/GaN and GaN/AlN nanoheterostructures with a cylindrical quantum wire in the semiconductor matrix of hexagonal crystals. At small QW radii ($R < 20 \text{ \AA}$), the contributions of all phonon branches to the polaron energy are commensurable. At $R > 20 \text{ \AA}$, the determinative contribution to the polaron energy is made by quasi-longitudinal confined phonons. At large R , the polaron effective mass is formed by quasi-longitudinal confined phonons, whereas, at small R , – by quasi-transverse interface and quasi-longitudinal confined phonons. The anisotropy of the crystals results in an increase of the polaron coupling energy.

1. N. Mori and T. Ando, Phys. Rev. B **40**, 6175 (1989).
2. M.H. Degani, Phys. Rev. B **40**, 11937 (1989).
3. Li Qiang and S. Das Sarma, Phys. Rev. B **40**, 5860 (1989).
4. N.V. Tkach and V.P. Zharkoi, Fiz. Tekhn. Polupr. **33**, 598 (1999).
5. M.V. Tkach, O.M. Makhanets', and I.V. Prots', Ukr. Fiz. Zh. **46**, 727 (2001).
6. H.J. Xie and X.Y. Liu, Superlatt. Microstruct. **39**, 489 (2006).
7. R.L. Rodriguez Suarez and A. Matos-Abiague, Physica E **18**, 485 (2003).
8. K.W. Sun, C.L. Huang, G.B. Huang, and H.C. Lee, Solid St. Commun. **126**, 519 (2003).
9. E.M. Höhberger, J. Kirschbaum, R.H. Blick, J.P. Kotthaus, and W. Wegscheider, Physica E, **18**, 99 (2003).
10. Y. Imanaka, H. Nojiri, Y.A. Matsuda, and N. Miura, Physica B **346-347**, 437 (2004).
11. H.C. Lee, K.W. Sun, and C.P. Lee, Solid St. Commun, **128**, 245 (2003).
12. You-Bin Yu, Kaang-Xian Guo, and Shi-Ning Zhu, Physica E **27**, 62 (2005).
13. R. Betancourt-Riera, R. Betancourt, R. Rosas, R. Riera, and J.L. Martin, Physica E, **24**, 257 (2004).

14. Li Zhang and Hong-Jing Xie, *Physica B* **363**, 146 (2005).
15. Li Zhang and Jun-jie Shi, *Semicond. Sci. Technol.* **20**, 592 (2005).
16. X.F. Wang and X.L. Lei, *Phys. Rev. B* **49**, 4780 (1994).
17. Hsu-Cheng Hsu and Wen-Feng Hsieh, *Phys. Rev. B* **40**, 11937 (1989).
18. S.M. Komirenko, K.W. Kim, M.A. Stroscio, and M. Dutta, *Phys. Rev. B* **59**, 5013 (1999).
19. A.D. Andreev and E.P. O'Reilly, *Phys. Rev. B* **62**, 15851 (2000).
20. Li Zhang and Jun-jie Shi, *Solid St. Commun.* **13**, 1 (2006).
21. D.E.N. Brancus and L.Ion, *Phys. Rev. B* **76**, 155304 (2007).
22. V.I. Boichuk, V.A. Borusevych, and I.S. Shevchuk, *J. Optoelectron. Adv. Mater.* **10**, 1357 (2008).
23. V.I. Boichuk, V.A. Borusevych, and I.S. Shevchuk, *Sensor Electron. Microsyst. Technol.* **3**, 11 (2008).
24. V.I. Boichuk, L.Ya. Voronyak, and Ya.M. Voronyak, *Fiz. Khim. Tverd. Tela* **11**, 34 (2010).
25. L. Zhang, *Superlatt. Microstruct.* **46**, 415 (2009).
26. L. Zhang, *Phys. Lett. A* **373**, 2087 (2009).

Received 15.12.10

Translated from Ukrainian by H.G. Kalyuzhna

ФОНОННИ ТА ПОЛЯРОННИ СТАНИ ЦИЛІНДРИЧНИХ ДРОТІВ ZnO/GaN ТА GaN/AlN

В.І. Бойчук, Л.Я. Вороняк, Я.М. Вороняк

Резюме

Для циліндричних квантових дротів (КД) кристалів гексагональної симетрії ZnO та GaN визначено залежності енергії поляризаційних фононів від хвильового вектора, а також енергії та ефективну масу полярона від радіуса КД (R). Показано, що основний внесок у основні параметри полярона (енергію та ефективну масу) задають квазіпоздовжні та інтерфейсні фононні моди. Встановлено, що в області $R > 15$ нм внесок квазіпоздовжніх фононів є основним. Проведено порівняння енергії полярона КД для кристалів кубічної та гексагональної симетрії.